J. Phys.: Condens. Matter **24** (2012) 265001 (7pp) doi:10.1088/0953-8984/24/26/265001

Thermal activation in atomic friction: revisiting the theoretical analysis

Y Dong[1], D Perez[2], H Gao[3] and A Martini[3]

[1] School of Mechanical Engineering, Purdue University, West Lafayette, IN 47907, USA
[2] Theoretical Division T-1, Los Alamos National Laboratory, Los Alamos, NM 87544, USA
[3] School of Engineering, University of California Merced, Merced, CA 95343, USA

E-mail: amartini@ucmerced.edu

Received 5 January 2012, in final form 30 April 2012
Published 29 May 2012
Online at stacks.iop.org/JPhysCM/24/265001

Abstract
The effect of thermal activation on atomic-scale friction is often described in the framework of the Prandtl–Tomlinson model. Accurate use of this model relies on parameters that describe the shape of the corrugation potential β and the transition attempt frequency f_0. We show that the commonly used form of β for a sinusoidal corrugation potential can lead to underestimation of friction, and that the attempt frequency is not, as is usually assumed, a constant value, but rather varies as the energy landscape evolves. We partially resolve these issues by demonstrating that numerical results can be captured by a model with a fitted β and using harmonic transition state theory to develop a variable form of the attempt frequency. We incorporate these developments into a more accurate and generally applicable expression relating friction to temperature and velocity. Finally, by using a master equation approach, we verify the improved analytical model is accurate in its expected regime of validity.

(Some figures may appear in colour only in the online journal)

1. Introduction

In atomic-scale friction, thermal effects play a significant role in helping nano-scale objects creep out from the energy barrier formed between two objects in relative motion [1, 2]. This creep motion due to thermal activation is responsible for the temperature and velocity dependence of friction which has been observed in both atomic force microscope (AFM) experiments [1, 3–5] and molecular dynamics (MD) simulation [6–9]. Thermal activation effects can also be described in the framework of the Prandtl–Tomlinson (PT) model [1–3]. The PT model [10, 11] is a reduced-order model that simplifies single asperity friction into a point mass (AFM tip) pulled via an elastic tether (cantilever) along a periodic potential energy profile (substrate). In this simple model, if there is no thermal activation, the point mass can slip to an adjacent potential well only when the energy barrier completely vanishes. With the help of thermal activation, however, the mass can overcome the energy barrier and slip earlier. The result is that friction decreases with temperature (more thermal energy and hence earlier slip) and increases with velocity (less time for thermal activation and hence later slip).

To enable theoretical analysis, the energy barrier takes the form [2, 3],

$$\Delta V = \frac{1}{\beta}(F_c - F)^{3/2}, \tag{1}$$

where F is the friction force, F_c is the friction force at the mechanical instability point (or critical point), and β is a parameter that reflects the shape of corrugation potential. This assumption is generally used (with others that will be discussed later) to yield the well-known relationship between friction force, temperature T and sliding velocity v,

$$\frac{1}{\beta k_B T}(F_c - F)^{3/2} = \ln\frac{v_0}{v} - \frac{1}{2}\ln\left(1 - \frac{F}{F_c}\right), \tag{2}$$

where k_B is the Boltzmann constant and v_0 is the critical velocity [1, 3]. The critical velocity is a function of attempt frequency f_0, which is usually assumed to be constant. For the frequently used sinusoidal corrugation potential, Riedo *et al*

found that $\beta = \frac{3\pi\sqrt{F_c}}{2\sqrt{2}a}$ using an asymptotic analysis [3]. This approach has been widely used to interpret frictional behavior observed in both simulations and experiments [4, 5, 7, 12–16].

In this paper, we show that the functional form of the commonly used expression for the energy barrier, given by equation (1), is adequate but that the value of β derived from the asymptotic analysis is inaccurate away from the critical point, which leads to an underestimation of the energy barrier. In addition, we show that the attempt frequency varies as the energy landscape evolves and that it can be obtained using harmonic transition state theory (HTST). The dependence of friction on temperature and velocity is re-examined using the variable attempt frequency f_0 and the more accurate β. Finally, a master equation method that requires a minimal number of assumptions is used to demonstrate that the improved analytical model is accurate enough to capture friction behavior except in the high-temperature and low-velocity regime, where back slip cannot be neglected.

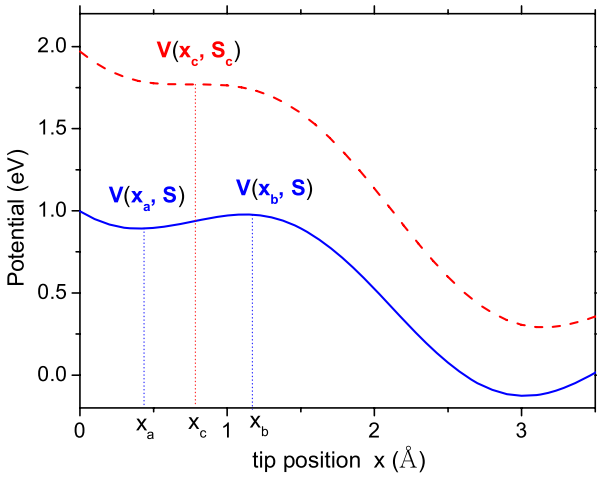

Figure 1. Illustration of the local minima x_a and saddle point x_b at support position S, as well as the critical point (x_c, S_c) where the energy barrier vanishes.

2. Corrugation potential shape

We begin with the mathematical formulation of the 1D PT model. The reduced-order PT model (an overview of this model and its various extensions can be found in [17]) simplifies the AFM tip/substrate system into a spring–mass system, whose total energy can be formulated as,

$$V(x, S) = U(x) + \tfrac{1}{2}k(S - x)^2. \tag{3}$$

The first term $U(x)$ on the right-hand side of this expression describes the corrugation potential. In most cases, it is assumed to have a sinusoidal form, $U(x) = -\frac{U_0}{2}\cos(\frac{2\pi x}{a})$, where U_0 is the amplitude, x is the tip position, and a is the lattice spacing of the substrate. The second term in equation (3) is the elastic potential resulting from the interaction between the tip and support, where k is the spring stiffness (or physically speaking the combined stiffness of the cantilever and tip) and $S = vt$ is the position of a support moving at a constant velocity v.

The dynamics of the tip can be described by the Langevin equation,

$$m\ddot{x} + m\mu\dot{x} = -\frac{\partial V(x, t)}{\partial x} + \xi(t), \tag{4}$$

where m is the mass of the tip, μ is the viscous friction (or damping) coefficient (more rigorously, μ is the damping coefficient per unit mass), and $\xi(t)$ is a Gaussian random force. In the following, we use $k = 1$ N m^{-1}, $a = 2.88$ Å, and $U_0 = 0.6$ eV. These parameters are consistent with those commonly reported for the PT model and are believed to have general relevance [17]. It has recently been argued that the effective mass should be that of the tip apex [18, 19]. However, in order to compare with previous theoretical work [1–3], we adopt the conventional effective mass, $m = 10^{-12}$ kg, which includes the cantilever and the main body of the tip. Note that this choice does not affect the applicability of the model, as changing the mass would simply rescale our results. We also want to point out here we will compute the static solution to obtain the energy barrier as well as the attempt frequency as a function of the friction force, so dynamic parameters such as temperature, sliding velocity and damping coefficient will not affect our numerical results. The procedure how to obtain the static equation is articulated below.

The total potential energy V as a function of tip position x is shown in figure 1. Given a support position S, the solution for the local minimum where the tip resides, x_a, and the transition point (or saddle point), x_b, can be determined from $\frac{\partial V}{\partial x} = 0$. Other variables can be obtained from these positions, such as the instantaneous friction force $F = k(S - x_a)$, the energy barrier $\Delta V = V(S, x_b) - V(S, x_a)$, and so on. As the support moves, S increases and the system approaches the so-called critical state where the energy barrier vanishes and the local minima x_a and saddle point x_b converge to a critical point x_c, as shown by the dashed line in figure 1. The critical point (x_c, S_c) is determined by $\frac{\partial V}{\partial x} = 0$ and $\frac{\partial^2 V}{\partial x^2} = 0$. These quantities can be obtained by numerically locating the energy minimum and saddle point, where we consider only static quantities such that dynamic parameters such as temperature and velocity do not affect the results.

This critical point can be used with the assumption that slip with the assistance of thermal activation occurs only in the vicinity of the critical point to obtain an analytical form of the corrugation potential shape parameter β. In this limit, the energy barrier between x_a and x_b can be expressed in the form of $\Delta V = \frac{1}{\beta}(F_c - F)^{3/2}$, where F_c is the friction force at the critical point (S_c, x_c) and F is the instantaneous friction force. For the specific case of a sinusoidal corrugation potential this analysis leads to the widely used expression, $\beta_{\sin} = \frac{3\pi\sqrt{F_c}}{2\sqrt{2}a}$ [3]; the derivation of β for an arbitrary potential is given in the appendix. It is worth noting that a linear form of the energy barrier $\Delta V = \frac{1}{\beta}(F_c - F)$ was first proposed in the pioneering work of Gnecco *et al* [1], followed by Sang *et al*, who showed the sub-linear three-halves law to be more rigorous [2]. Although it is not easy to differentiate the sub-linear from the linear relationship under current experimental conditions [20], we expect that

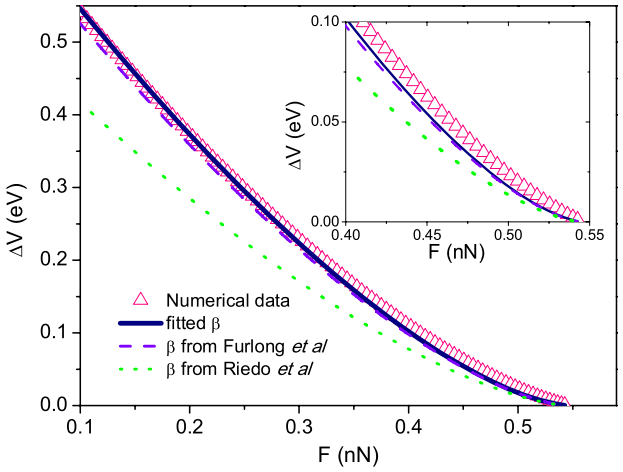

Figure 2. Comparison of the energy barrier obtained by numerical solution (triangles) to predictions of the analytical model (equation (1)) with β given by Riedo *et al* [3] (dotted line), reported by Furlong *et al* [21] (dashed line), and fitted to the analytical equation using the numerical data (solid line).

this distinction may become more obvious as additional experimental temperature dependence data becomes available and at higher scanning speeds.

We can now evaluate the accuracy of the analytical model through a comparison to the energy barrier obtained by numerically locating the saddle point under static conditions. Figure 2 shows that the analytical model with $\beta_{\sin} = \frac{3\pi\sqrt{F_c}}{2\sqrt{2}a}$ substantially underestimates the energy barrier. However, if we instead consider β as a fitting parameter, $\Delta V = \frac{1}{\beta}(F_c - F)^{3/2}$ provides an adequate description of the barrier variation over a large range of forces. This issue was also recently identified by Furlong *et al* [21] when fitting a friction versus velocity curve to Monte Carlo simulations. They too found that equation (1) was applicable when used with a semi-empirical value of $\beta = \frac{F_c^{3/2}}{\frac{C_{\text{eff}}a^2}{8} + \frac{F_c a}{\pi}}$, where C_{eff} is an effective stiffness. Here we supplement that work by showing that the origin of the limitation in the typically used form of β is the assumption that slip occurs near the critical point; this assumption is reflected in the derivation given in the appendix as neglecting higher order terms in the Taylor expansion taken around the critical point.

3. Variable attempt frequency

Within harmonic transition state theory (HTST), the probability p that the tip resides in the initial local minimum (in the absence of back slips) can be obtained by solving:

$$\frac{dp}{dt} = -f_0 \exp\left(\frac{-\Delta V}{k_B T}\right) p, \tag{5}$$

where f_0 is the attempt frequency, ΔV is the energy barrier, k_B is the Boltzmann constant and T is the temperature. In most previous works [1, 22, 3], f_0 was assumed to be constant. In reality, however, the attempt frequency varies with the support position $S(t)$, because the vibrational frequency of the tip is affected by the curvature of the potential well in which it resides. This suggests that the use of a constant attempt frequency may lead to inaccuracies.

A good approximation to the attempt frequency can be obtained from the HTST [23],

$$f_0 = \frac{1}{2\pi} \frac{\prod_{i=1}^{N} \lambda_i^{(a)}}{\prod_{j=1}^{N-1} \lambda_j^{(b)}}, \tag{6}$$

where the $(\lambda_i^{(a)})^2$ and $(\lambda_j^{(b)})^2$ are the positive normal-mode eigenvalues of the Hessian matrix at the minimum a and saddle point b of V, respectively.

Then for a one-spring PT model, the attempt frequency can be written as

$$f_0 = \frac{w_a}{2\pi}, \tag{7}$$

where $w_a = \sqrt{\frac{V_{xx}(x_a, S)}{m}}$ is the angular frequency at the local minimum a, and m is the effective mass.

The Taylor expansion suggests the following form of the attempt frequency,

$$f_0 = \gamma (F_c - F)^{\alpha}, \tag{8}$$

where γ and α are parameters to be determined. We also assume that slip occurs around the critical point (x_c, S_c), so $V_{xx}(x_a, S)$ can be obtained by Taylor expansion around the critical point,

$$\begin{aligned} V_{xx}(x_a, S) = {} & V_{xx}(x_c, S_c) + V_{xxx}(x_a - x_c) \\ & + V_{xxS}(S - S_c) + O(\delta x^2). \end{aligned} \tag{9}$$

Revisiting equation (3) at the critical point (x_c, S_c), we obtain $V_{xx}(x_c, S_c) = 0$ and $V_{xxS} = 0$, and end up with

$$V_{xx}(x_a, S) = U_{xxx}(x_a - x_c), \tag{10}$$

where the subscript $_{xx}$ indicates a second derivative with respect to x, with similar notation for higher derivatives. Using equations (A.3) and (A.7) in the appendix, and substituting equation (10) into (7), we obtain,

$$f_0 = \frac{1}{2\pi\sqrt{m}} (-2U_{xxx})^{1/4} (F_c - F)^{1/4}. \tag{11}$$

For any corrugation potential with finite third derivatives, the coefficients of equation (8) are $\gamma = \frac{1}{2\pi\sqrt{m}}(-2U_{xxx})^{1/4}$ and $\alpha = 1/4$; for a sinusoidal potential $\gamma = \frac{1}{2\pi\sqrt{m}}(\frac{8\pi^2 F_c}{a^2})^{1/4}$. Figure 3 presents a comparison of the attempt frequency computed numerically around the exact x_a to the prediction of the analytical model for a sinusoidal potential. The results show that the analytical expression produces a good approximation of the attempt frequency across a wide range of friction forces.

The harmonic transition state theory (HTST) used in this work neglects the effect of damping and gives an upper bound for the real attempt frequency. The effect of the damping on attempt frequency in the PT model can be obtained, but has a more complicated form [23]. For example, for an

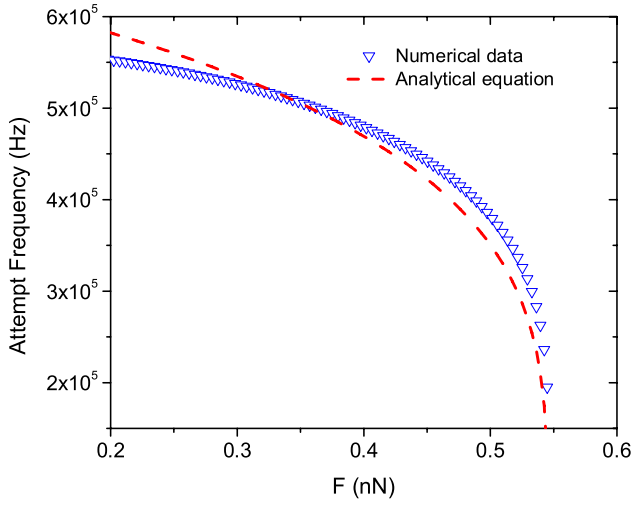

Figure 3. Comparison of the analytical expression for the variation of attempt frequency with friction (equation (11)) to numerical data for a sinusoidal corrugation potential.

over-damped system, the attempt frequency can be expressed as

$$f_0 = \frac{w_a w_b}{2\pi\mu}, \tag{12}$$

where w_a and w_b are the angular frequencies at the local minimum a and saddle point b, respectively, and μ is the damping coefficient. The frequencies at the minimum and saddle can again be obtained by taking a Taylor expansion of the total potential around the critical point. The resultant expression for the angular frequencies w_a and w_b can be substituted into equation (12). Using the relationship between friction and support position, we have the following form of the attempt frequency for an over-damped system:

$$f_0 = \frac{1}{2\pi m\mu}(-2U_{xxx})^{1/2}(F_c - F)^{1/2}. \tag{13}$$

So, for an over-damped system, the coefficients of equation (8) are $\gamma = \frac{1}{2\pi m\mu}(-2U_{xxx})^{1/2}$ and $\alpha = \frac{1}{2}$.

Note that the derivation of the variable attempt frequency is, like that for the analytical form of β, based on the assumption that slip occurs near the critical point. However, the effect of this assumption on attempt frequency is less significant than its effect on β (and hence on the energy barrier), because the transition rate, equation (5), (which directly affects friction) is an exponential function of the energy barrier, but only a linear function of attempt frequency.

4. Velocity and temperature dependence of friction

With the energy barrier ΔV and attempt frequency f_0 as functions of $(F_c - F)$, we can revisit equation (5). First, we replace the left-hand side of equation (5) with

$$\frac{dp}{dt} = \frac{dp}{dF}\frac{dF}{dt}. \tag{14}$$

We also have $F = C_{\text{eff}}S$, which is an empirical relation and can be observed both in experiments and simulations. In a typical stick–slip friction curve, the friction in the 'stick' period increases linearly with the support displacement S, and the linear coefficient C_{eff} is the total effective stiffness of the system including the cantilever, tip and contact stiffness. Assuming that the support moves at a constant velocity v, we have

$$\frac{dF}{dt} = C_{\text{eff}}\frac{dS}{dt} = C_{\text{eff}}v. \tag{15}$$

Substituting equations (14) and (15) into (5),

$$\frac{dp}{dF} = -\frac{f_0}{C_{\text{eff}}v}\exp\left(\frac{-\Delta V}{k_B T}\right)p. \tag{16}$$

Using the condition for maximum probability of slip $\frac{d^2p}{dF^2} = 0$ with equations (1) and (8) we obtain a new relation for $F(v, T)$,

$$\frac{1}{\beta k_B T}(F_c - F)^{3/2} = \ln\frac{v_0}{v} + \ln M - \left(\frac{1}{2} - \alpha\right) \times \ln\left(1 - \frac{F}{F_c}\right), \tag{17}$$

where $M = (1 - \frac{2\alpha\beta k_B T}{3(F_c - F)^{3/2}})^{-1}$ has a value near unity such that $\ln M$ can be neglected. The critical velocity has the form,

$$v_0 = \frac{2\gamma F_c^{\alpha}\beta k_B T}{3C_{\text{eff}}\sqrt{F_c}}. \tag{18}$$

Now we can evaluate $F(v, T)$ for different attempt frequencies. For a system subject to HTST, where $\gamma = \frac{1}{2\pi\sqrt{m}}(-2U_{xxx})^{1/4}$ and the exponent $\alpha = \frac{1}{4}$, the velocity and temperature dependence of friction can be expressed as

$$\frac{1}{\beta k_B T}(F_c - F)^{3/2} = \ln\frac{v_0}{v} - \frac{1}{4}\ln\left(1 - \frac{F}{F_c}\right). \tag{19}$$

Note that this expression differs from the commonly used form (equation (2)) in that the critical velocity is slightly different and that the term $\ln(1 - \frac{F}{F_c})$ is multiplied by 1/4 instead of 1/2. If we assume $f_0 = \gamma F_c^{\alpha}$, we can isolate the effect of attempt frequency, as shown in figure 4. This analysis reveals that in the low-velocity regime the results are almost indistinguishable, while at higher velocities the constant attempt frequency assumption underestimates the average friction.

Finally, we also consider the over-damped limit. For this case we showed that $\alpha = \frac{1}{2}$ and $\gamma = \frac{1}{2\pi m\mu}(-2U_{xxx})^{1/2}$, from which we obtain an expression for friction in an over-damped system,

$$\frac{1}{\beta k_B T}(F_c - F)^{3/2} = \ln\frac{v_0}{v}. \tag{20}$$

Interestingly, we recover the result of Sang *et al* [2], who also worked in the over-damped limit. We note, however, that, although damping in an AFM tip/substrate system is still controversial, evidence suggests that it is likely somewhere between the limiting cases of under-damped ($\mu < w_b$) and over-damped ($\mu \geq w_b$) [24, 25], i.e. a system in the over-damped limit ($\mu \gg w_b$) is rare. Close to critical damping, HTST offers a very good approximation to the true transition

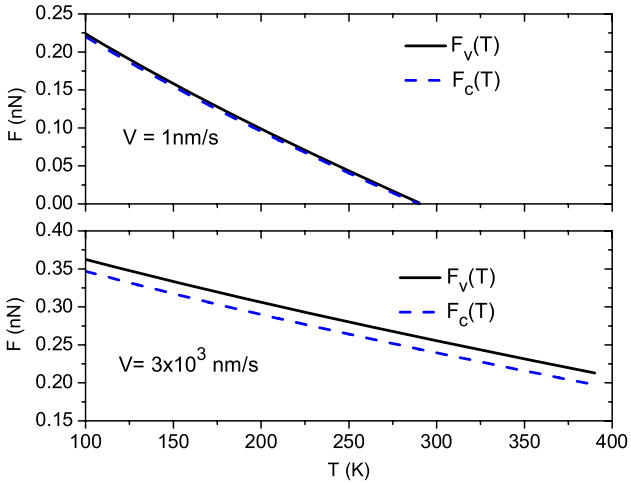

Figure 4. Average friction as a function of temperature at two different sliding velocities. $F_v(T)$ is obtained using a variable attempt frequency and $F_c(T)$ is obtained assuming a constant attempt frequency.

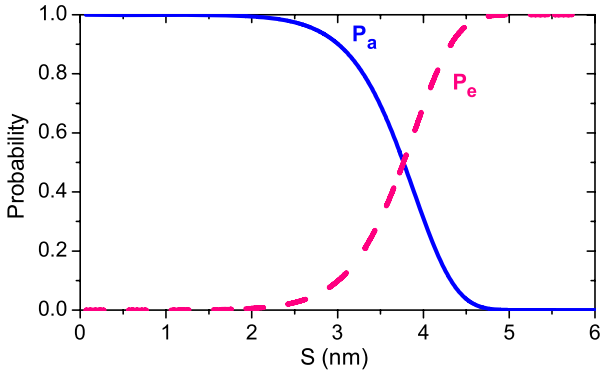

Figure 5. The evolution of the probability of the tip residing in state a (solid line) and e (dashed line) with support position; $T = 300$ K and $v = 10^3$ nm s^{-1}.

rate, so we will, from here on, rely on the HTST attempt frequency.

5. Master equation method

The commonly used expression relating friction to temperature and velocity, equation (2), is based on several assumptions: (i) slip occurs in the vicinity of the critical point, (ii) only single, forward slips occur, (iii) the contact stiffness is much larger than the cantilever/tip stiffness, (iv) the energy barrier has the form $\Delta V = \frac{1}{\beta}(F_c - F)^{3/2}$, (v) the analytically derived form of $\beta = \frac{3\pi\sqrt{F_c}}{2\sqrt{2}a}$ is accurate, and (vi) the attempt frequency is constant. We have shown in previous sections that the assumptions regarding β and the attempt frequency can lead to errors, and these assumptions can be avoided by fitting β directly to numerical data and applying HTST to identify a variable form of the attempt frequency. However, our improved methods still rely upon the first four assumptions. Therefore, we here present another approach using the master equation method, which yields predictions of the velocity and temperature dependence of friction while requiring fewer assumptions [9, 26]. This approach, in which a set of master equations is used to describe the dynamics of transitions between states, requires only two assumptions: only single slip occurs, and HTST applies.

Consider that the tip resides in state a initially and slips to state e with the help of external driving as well as thermal activation. The probability of residing in a given state can be written as

$$\begin{aligned} \frac{dP_a}{dt} &= k_{e\to a}P_e - k_{a\to e}P_a \\ \frac{dP_e}{dt} &= k_{a\to e}P_a - k_{e\to a}P_e, \end{aligned} \tag{21}$$

where $k_{e\to a}$ is the instantaneous transition rate from state e to state a, and $k_{a\to e}$ is the instantaneous transition rate from state a to state e. Both of them vary with the support displacement $S = vt$. The transition rates can be determined using HTST theory described by equation (7). When $S(t = 0) = 0$, we set the initial conditions as $P_a(0) = 1$ and $P_e(0) = 0$ such that the tip begins at state a. We then apply the Runge–Kutta method to solve for P_a and P_e. Figure 5 illustrates the evolution of the probability of the tip residing in states a and e with the displacement of the support. Note that back slips are here taken into account, since transition state theory is applied at both energy minima (forward slip from a to e, and back slip from e to a).

Once the time-dependent probability of occupying each state is determined, physical quantities can be obtained as weighted averages over the different states. For example, the instantaneous friction $F(t)$ can be written as

$$F(t) = \sum F_i P_i, \tag{22}$$

where F_i and P_i are the force and occupation probability in state i, respectively. Using this we can obtain the average friction corresponding to various velocities and temperatures.

Finally, to illustrate the overall effect of the derivations presented in this paper, we plot friction as a function of velocity and temperature in figure 6. $F_1(v, T)$ is obtained from the master equation method which requires the fewest assumptions and so is believed to produce the most accurate result, $F_2(v, T)$ is the analytical prediction with variable attempt frequency and fitted β, and $F_3(v, T)$ is the analytical prediction with variable attempt frequency and $\beta = \frac{3\pi\sqrt{F_c}}{2\sqrt{2}a}$. This figure shows that the prediction based on the analytical form of β, $F_3(v, T)$, underestimates friction at all temperatures and velocities. This is expected since, as mentioned earlier, the transition rate is exponentially related to the energy barrier, which we showed was underestimated using $\beta = \frac{3\pi\sqrt{F_c}}{2\sqrt{2}a}$. The analytical expression using a fitted β, $F_2(v, T)$, does a much better job at capturing the frictional behavior. The exception to this is in the high-temperature and low-velocity regime, where it fails to capture the plateau exhibited by $F_1(v, T)$. At high temperature and low velocity, the occurrence of back slips will lead to thermolubricity [28, 27]; the transition between the two regions is discussed

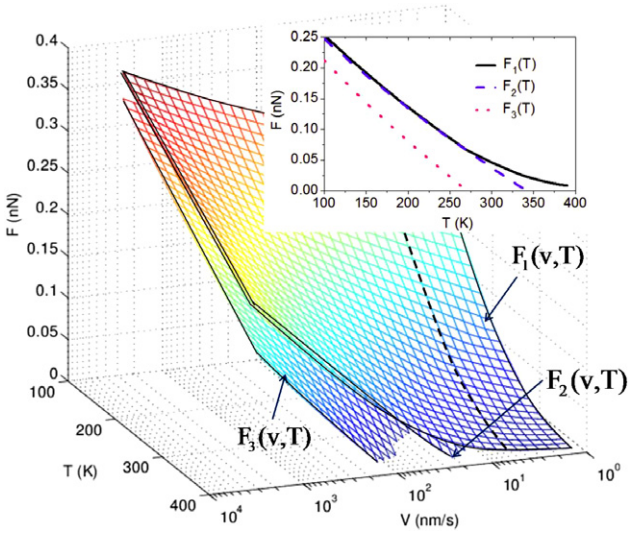

Figure 6. Variation of average friction with velocity and temperature calculated illustrating the impact of the derivations presented in this paper. F_1: master equation method, F_2: attempt frequency from HTST and with a fitted β, F_3: attempt frequency from HTST with $\beta_{\sin} = \frac{3\pi\sqrt{F_c}}{2\sqrt{2}a}$. Inset is a plot of friction versus temperature corresponding to the dashed line at constant velocity.

in [25]. Since the analytical model is based on the assumption that there are no back slips, it cannot reproduce the friction behavior in the thermolubricity regime.

6. Conclusion

We re-examined the velocity and temperature dependence of friction in the framework of the Prandtl–Tomlinson model with thermal activation. First, we showed that the form of β obtained from asymptotic analysis underestimates the energy barrier and can thus lead to a substantial underestimation of friction. However, we also showed that, although that β leads to inaccurate results, the relation $\Delta V = \frac{1}{\beta}(F_c - F)^{3/2}$ still holds true and a fitted β can be used to obtain more accurate predictions. Secondly, a variable attempt frequency f_0 of the form $\gamma(F_c - F)^{\alpha}$ was proposed. For a system subject to harmonic transition state theory, we found $\gamma = \frac{1}{2\pi\sqrt{m}}(-2U_{xxx})^{1/4}$ and $\alpha = \frac{1}{4}$. Using the fitted β and a variable attempt frequency, we derived a modified expression relating friction to temperature and velocity. By direct comparison to the result of a master equation approach based on few assumptions, we showed that friction predicted using the new analytical equation is accurate except in the high-temperature and low-velocity regime, where back slip can no longer neglected.

Acknowledgments

This work was motivated by discussions with Dr R W Carpick regarding the accuracy of $\beta_{\sin}$. AM and YD thank the National Science Foundation for its support through award CMMI-1068552 and AM thanks the Air Force Office of Sponsored Research for support through award FA9550-12-1-0221. Work at Los Alamos National Laboratory (LANL) was supported by the United States Department of Energy (US DOE) Office of Basic Energy Sciences, Materials Sciences and Engineering Division. LANL is operated by Los Alamos National Security, LLC, for the National Nuclear Security Administration of the US DOE under Contract No. DE-AC52-06NA25396.

Appendix. Corrugation potential shape β

The following details the use of an asymptotic method to rigorously derive the corrugation potential shape parameter β for an arbitrary corrugation potential. To obtain the form of β, we first develop an expression relating the energy barrier ΔV to the difference between friction with and without thermal activation, $(F_c - F)$. As illustrated in figure 1, the energy barrier ΔV can be calculated by $\Delta V = V(x_b, S) - V(x_a, S)$ given a support position S. Using the assumption that slip with the assistance of thermal activation occurs in the vicinity of the critical point (x_c, S_c), the corresponding system potential $V(x, S)$ can be obtained from a Taylor expansion around (x_c, S_c) [22, 25]:

$$\begin{aligned} V(x,S) = {} & V(x_c,S_c) + \frac{\partial V}{\partial x}(x-x_c) + \frac{\partial V}{\partial S}(S-S_c) \\ & + \frac{\partial^2 V}{\partial x \partial S}(x-x_c)(S-S_c) + \frac{1}{2}\frac{\partial^2 V}{\partial x^2}(x-x_c)^2 \\ & + \frac{1}{2}\frac{\partial^2 V}{\partial S^2}(S-S_c)^2 + \frac{1}{6}\frac{\partial^3 V}{\partial x^3}(x-x_c)^3 \\ & + \frac{1}{6}\frac{\partial^3 V}{\partial S^3}(S-S_c)^3 \\ & + \frac{1}{2}\frac{\partial^3 V}{\partial x^2 \partial S}(x-x_c)^2(S-S_c) \\ & + \frac{1}{2}\frac{\partial^3 V}{\partial x \partial S^2}(x-x_c)(S-S_c)^2 + \mathrm{O}(\delta x^4). \end{aligned} \quad (A.1)$$

Then, since $\frac{\partial V}{\partial x} = 0$ at the local minimum x_a or the saddle point x_b, we can set the derivative of equation (A.1) with respect to x to zero. Using equation (3), this yields the following relationship between $(S_c - S)$ and $(x_c - x)$ at a minimum or saddle point,

$$(S_c - S) = \frac{U_{xxx}}{-2k}(x - x_c)^2, \quad (A.2)$$

where the notation U_{xxx} indicates the third derivative of U with respect to x at the critical point x_c.

For a given S, where $S < S_c$, the local minima x_a is smaller than x_c and the saddle point x_b is larger than x_c. Thus we have two relations:

$$\begin{aligned} (x_a - x_c) &= -\sqrt{\frac{-2k}{U_{xxx}}}(S_c - S)^{1/2} \\ (x_b - x_c) &= +\sqrt{\frac{-2k}{U_{xxx}}}(S_c - S)^{1/2}. \end{aligned} \quad (A.3)$$

After substituting equation (A.3) into (A.1), canceling terms with $\frac{\partial V}{\partial x} = 0$ and $\frac{\partial^2 V}{\partial x^2} = 0$, and neglecting higher order terms

of $(S_c - S)^\eta$ where $\eta > \frac{3}{2}$, we have:

$$\begin{aligned} V(x_b, S) &\simeq V(x_c, S_c) - \frac{\partial V}{\partial S}(S_c - S) \\ &\quad + \tfrac{2\sqrt{2}}{3}k^{3/2}(-U_{xxx})^{-1/2}(S_c - S)^{3/2} \\ V(x_a, S) &\simeq V(x_c, S_c) - \frac{\partial V}{\partial S}(S_c - S) \\ &\quad - \tfrac{2\sqrt{2}}{3}k^{3/2}(-U_{xxx})^{-1/2}(S_c - S)^{3/2}. \end{aligned} \tag{A.4}$$

The energy barrier $\Delta V = V(x_b, S) - V(x_a, S)$ can then be calculated as

$$\Delta V = \frac{4\sqrt{2}}{3}k^{3/2}(-U_{xxx})^{-1/2}(S_c - S)^{3/2}. \tag{A.5}$$

Next, since $F = k(S - x)$, we have:

$$F_c - F = k(S_c - x_c) - k(S - x_a). \tag{A.6}$$

Assuming that the contact stiffness is much larger than the stiffness of the combination the tip and cantilever [3] (which is reasonable for a real AFM system where the stiffness of the tip apex is believed to be on the order of 1 N m^{-1} [29]), $S_c - S$ is much larger than $x_c - x_a$, so that

$$F_c - F \simeq k(S_c - S). \tag{A.7}$$

Then, substituting equation (A.7) into (A.5) we have

$$\Delta V = \frac{4\sqrt{2}}{3}(-U_{xxx})^{-1/2}(F_c - F)^{3/2}. \tag{A.8}$$

Recalling the expression $\Delta V = \frac{1}{\beta}(F_c - F)^{3/2}$, this means that β, which reflects the shape of the corrugation potential between the tip and substrate, has a general form

$$\beta = \frac{3}{4\sqrt{2}}\sqrt{-U_{xxx}}. \tag{A.9}$$

For the specific case of a sinusoidal corrugation potential $U = -\frac{1}{2}U_0\cos(\frac{2\pi x}{a})$, we obtain the commonly used form of β,

$$\beta_{\sin} = \frac{3\pi}{2\sqrt{2}a}\sqrt{\frac{\pi U_0}{a}\sin\frac{2\pi x_c}{a}} = \frac{3\pi\sqrt{F_c}}{2\sqrt{2}a}. \tag{A.10}$$

References

[1] Gnecco E, Bennewitz R, Loppacher C, Bammerlin M, Meyer E and Guntherodt H J 2000 Velocity dependence of atomic friction *Phys. Rev. Lett.* **84** 1172

[2] Sang Y, Dube M and Grant M 2001 Thermal effects on atomic friction *Phys. Rev. Lett.* **87** 174301

[3] Riedo E, Gnecco E, Bennewitz R, Meyer E and Brune H 2003 Interaction potential and hopping dynamics governing sliding friction *Phys. Rev. Lett.* **91** 084502

[4] Jansen L, Hölscher H, Fuchs H and Schirmeisen A 2010 Temperature dependence of atomic-scale stick–slip friction *Phys. Rev. Lett.* **104** 256101

[5] Li Q, Dong Y, Perez D, Martini A and Carpick R W 2011 Speed dependence of atomic stick–slip friction in optimally matched experiments and molecular dynamics simulations *Phys. Rev. Lett.* **106** 126101

[6] Mishin Y, Suzuki A, Uberuaga B P and Voter A F 2007 Stick-slip behavior of grain boundaries studied by accelerated molecular dynamics *Phys. Rev.* B **75** 224101

[7] Martini A, Dong Y, Perez D and Voter A F 2009 Low-speed atomistic simulation of stick–slip friction using parallel replica dynamics *Tribol. Lett.* **36** 63

[8] Kim W K and Falk M L 2010 Accelerated molecular dynamics simulation of low-velocity frictional sliding *Modelling Simul. Mater. Sci. Eng.* **18** 034003

[9] Perez D, Dong Y, Martini A and Voter A F 2010 Rate theory description of atomic stick–slip friction *Phys. Rev.* B **81** 245415

[10] Prandtl L 1928 Hypothetical model for the kinetic theory of solid bodies *Z. Angew. Math. Mech.* **8** 85

[11] Tomlinson G A 1929 A molecular theory of friction *Phil. Mag.* **7** 905

[12] Riedo E and Gnecco E 2004 Thermally activated effects in nanofriction *Nanotechnology* **15** S288

[13] Tambe N S and Bhushan B 2005 Friction model for the velocity dependence of nanoscale friction *Nanotechnology* **16** 2309

[14] Chen J, Ratera I, Park J Y and Salmeron M 2006 Velocity dependence of friction and hydrogen bonding effects *Phys. Rev. Lett.* **96** 236102

[15] Schirmeisen A, Jansen L, Hölscher H and Fuchs H 2006 Temperature dependence of point contact friction on silicon *Appl. Phys. Lett.* **88** 123108

[16] Brukman M J, Gao G, Nemanich R J and Harrison J A 2008 Temperature dependence of single-asperity diamond–diamond friction elucidated using AFM and MD simulations *J. Phys. Chem.* C **112** 9358

[17] Dong Y, Vadakkepatt A and Martini A 2011 Analytical models for atomic friction *Tribol. Lett.* **44** 367

[18] Krylov S Y, Dijksman J A, vanLoo W A and Frenken J W M 2006 Stick–slip motion in spite of a slippery contact: do we get what we see in atomic friction? *Phys. Rev. Lett.* **97** 166103

[19] Dong Y, Gao H and Martini A 2012 Suppression of atomic friction under cryogenic conditions: the role of athermal instability in AFM measurements *Europhys. Lett.* **98** 16002

[20] Sills S and Overney R M 2003 Creeping friction dynamics and molecular dissipation mechanisms in glassy polymers *Phys. Rev. Lett.* **91** 95501

[21] Furlong O J, Manzi S J, Pereyra V D, Bustos V and Tysoe W T 2009 Kinetic Monte Carlo theory of sliding friction *Phys. Rev.* B **80** 153408

[22] Persson B N J, Albohr O, Mancosu F, Peveri V, Samoilov V N and Sivebæk I M 2003 On the nature of the static friction, kinetic friction and creep *Wear* **254** 835

[23] Hanggi P, Talkner P and Borkovec M 1990 Reaction-rate theory: fifty years after Kramers *Rev. Mod. Phys.* **62** 251

[24] Roth R, Glatzel T, Steiner P, Gnecco E, Baratoff A and Meyer E 2010 Multiple slips in atomic-scale friction: an indicator for the lateral contact damping *Tribol. Lett.* **39** 63

[25] Müser M H 2011 Velocity dependence of kinetic friction in the Prandtl–Tomlinson model *Phys. Rev.* B **84** 125419

[26] Braun O M and Peyrard M 2010 Master equation approach to friction at the mesoscale *Phys. Rev.* E **82** 036117

[27] Müser M H 2002 Nature of mechanical instabilities and their effect on kinetic friction *Phys. Rev. Lett.* **89** 224301

[28] Jinesh K B, Krylov S Y, Valk H, Dienwiebel M and Frenken J W M 2008 Thermolubricity in atomic-scale friction *Phys. Rev.* B **78** 155440

[29] Reimann P and Evstigneev M 2005 Description of atomic friction as forced Brownian motion *New J. Phys.* **7** 25